

INVESTIGATION OF LATTICE CONSTANTS AND ELASTIC MODULI OF YTTRIA-DOPED CERIA CRYSTAL BY STATISTICAL MOMENT METHOD

Dang Thanh Hai^{1(*)}, Vu Van Hung², Le Thi Thanh Huong³, Le Thu Lam⁴

¹Vietnam Education Publishing House, ²University of Education - VNU,

³Hai Phong University, ⁴Tay Bac University

Abstract: *In the present study, we developed a formalism based on the statistical moment method to investigate lattice constant and elastic moduli of yttria-doped ceria crystal including the anharmonicity effects of thermal lattice vibrations. The lattice constant and elastic moduli are calculated as functions of the dopant concentration, temperature, and pressure. We calculate the elastic moduli under temperature up to 1800K and pressure up to 60GPa using Buckingham potential. Our calculations are compared with theoretical and experimental results.*

Keywords: *Lattice constant, elastic moduli, yttria-doped ceria crystal.*

Received 25 June 2021

Revised and accepted for publication 23 August 2021

(*) Email: haiphysic@gmail.com

1. INTRODUCTION

Pure ceria (CeO_2) electrolyte is not a good oxygen ion conductor. There are very few oxygen vacancies in ceria due to the high vacancy formation energy. Because of Y^{3+} ion of lower charge than the host cation, the substitution of Ce^{4+} by Y^{3+} ions creates many oxygen vacancies to maintain overall charge neutrality in the crystal lattice [3, 14, 10, 25]. Yttria-doped ceria (YDC) crystal is a well-known oxygen ion conductor and a very relevant material as an electrolyte in solid oxide fuel cells (SOFCs). With the fluorite structure, the presence of the oxygen vacancies allows the oxygen ions to be extracted (or inserted into) the lattice sites of YDC crystal in a low-oxygen (or oxygen-rich) environment, respectively [4].

A large number of experimental and theoretical studies have been carried out on catalytic [19], lattice vibrational [13], structural [26] and mechanical properties [21] of cerium dioxides. Theoretical study on the structure, stability and, morphology of stoichiometric ceria crystallines has been done using the simulation method [20]. The change

in cubic lattice constant of YDC crystal as a function dopant concentration obtained from the molecular dynamics (MD) simulation and previous X-ray diffraction (XRD) experiment at 300K and zero external pressure [2]. However, the dependence of lattice constant on the pressure has not been evaluated in detail. In a recent study, E. Wachtel and I. Lubomirsky [21] measured the elastic modulus of pure and doped ceria to understand the mechanical behavior under doping level and oxygen vacancy concentration. They found that the presence of oxygen vacancies makes the chemical bonds “softer” and the measured value depends strongly on the measurement technique and the thermal history of the sample. It is noted that elastic properties play an important role in controlling crystallization of amorphous phases, and the stiffness of the chemical bonds can be reflected by the elastic modulus [17]. Notwithstanding, the anharmonicity of lattice vibrations has been neglected in most of the previous theoretical studies related to the lattice constant and elastic moduli of YDC crystal.

The present work attempts to provide an overview of the lattice constant and elastic moduli of YDC crystal. The lattice constant, Young’s, bulk, and shear moduli are calculated in detail at various dopant concentrations, temperature, and pressure using the statistical moment method (SMM). The analytic expressions of lattice constant and elastic moduli are derived taking into account the anharmonicity effects of the lattice vibrations. The present calculations are compared with the previous theoretical calculations as well as with the available experimental results.

2. BODY

2.1. Theory

YDC crystal has the fluorite structure where O^{2-} ions occupy the fcc sites and Ce^{4+} and Y^{3+} ions occupy the tetrahedral interstitial sites. Due to Y^{3+} ions of lower charge than the host cations, an oxygen vacancy is generated for every two Y^{3+} ions [16]. Let us consider YDC crystal with N_{Ce} Ce^{4+} ions, N_Y Y^{3+} ions, N_O O^{2-} ions and N_{va} oxygen vacancies. The number of cations and yttrium concentration in YDC crystal are denoted by N and x , respectively, then $N_{Ce} = N(1-x)$, $N_Y = Nx$, $N_O = N(2-x/2)$ and $N_{va} = Nx/2$. Hence, the formulation of YDC crystal is written as $Ce_{1-x}Y_xO_{2-x/2}$.

Using the Boltzmann relation, the Helmholtz free energy of $Ce_{1-x}Y_xO_{2-x/2}$ system can be written by taking into account the configuration entropy of system, S_c^* [8, 9]

$$\Psi = \Psi_{CeO_{2-x/2}} + \Psi_Y - N_Y u_0^{Ce} - TS_c^*, \quad (1)$$

with u_0^{Ce} is the average interaction potential of a Ce^{4+} ion in $CeO_{2-x/2}$ system, $\Psi_{CeO_{2-x/2}}$ is the Helmholtz free energy of $CeO_{2-x/2}$ system, Ψ_Y is the Helmholtz free energy of Y^{3+} ions,

$$\Psi_{CeO_{2-x/2}} = C_{Ce} \Psi_{Ce} + C_O \Psi_O - TS_c, \quad (2)$$

$$\begin{aligned} \Psi_Y = & U_0^Y + \Psi_0^Y + 3N_Y \left\{ \frac{\theta^2}{k_Y^2} \left[\gamma_Y^2 X_Y^2 - \frac{2\gamma_Y^1}{3} a_1^Y \right] + \right. \\ & \left. + \frac{2\theta^3 a_1^Y}{k_Y^4} \left[\frac{4}{3} (\gamma_2^Y)^2 X_Y - 2 \left((\gamma_1^Y)^2 + 2\gamma_1^Y \gamma_2^Y \right) (2a_1^Y - 1) \right] \right\}, \end{aligned} \quad (3)$$

here, C_{Ce} , C_O are the concentrations of Ce^{4+} and O^{2-} ions in $CeO_{2-x/2}$ system, respectively, $C_{Ce} = x/3$, $C_O = (2-x/2)/3$, and Ψ_{Ce} , Ψ_O are the Helmholtz free energies of Ce^{4+} , O^{2-} ions in $CeO_{2-x/2}$ system, respectively,

$$\begin{aligned} \Psi_{Ce} = & U_0^{Ce} + \Psi_0^{Ce} + 3N_{Ce} \left\{ \frac{\theta^2}{k_{Ce}^2} \left[\gamma_{Ce}^2 X_{Ce}^2 - \frac{2\gamma_{Ce}^1}{3} a_1^{Ce} \right] \right. \\ & \left. + \frac{2\theta^3 a_1^{Ce}}{k_{Ce}^4} \left[\frac{4}{3} (\gamma_2^{Ce})^2 X_{Ce} - 2 \left((\gamma_1^{Ce})^2 + 2\gamma_1^{Ce} \gamma_2^{Ce} \right) (2a_1^{Ce} - 1) \right] \right\}, \end{aligned} \quad (4)$$

$$\begin{aligned} \Psi_O = & U_0^O + \Psi_0^O + 3N_O \left\{ \frac{\theta^2}{k_O^2} \left[\gamma_O^2 X_O^2 - \frac{2\gamma_O^1}{3} a_1^O \right] \right. \\ & \left. + \frac{2\theta^3 a_1^O}{k_O^4} \left[\frac{4}{3} (\gamma_2^O)^2 X_O - 2 \left((\gamma_1^O)^2 + 2\gamma_1^O \gamma_2^O \right) (2a_1^O - 1) \right] \right\} \\ & + 3N_O \left\{ \frac{\theta\beta}{6K\gamma_O} \left(\frac{k_O}{K} - 1 \right) + \frac{\theta^2\beta}{K} \left[\left(\frac{2\gamma_O a_1^O}{3K^3} \right)^{\frac{1}{2}} - \frac{\beta a_1^O}{9K^2} + \frac{\beta k_O a_1^O}{9K^3} + \frac{\beta}{6Kk_O} (X_O - 1) \right] \right\}. \end{aligned} \quad (5)$$

In Eqs. (3), (4), (5), the parameters $k_{Ce,O,Y}$, $x_{Ce,O,Y}$, x_Y , $a_1^{Ce,O,Y}$, β , K , $\gamma_1^{Ce,O,Y}$, $\gamma_2^{Ce,O,Y}$, $\gamma_{Ce,O,Y}$ are defined as Refs. [8, 9], and Ψ_0^{Ce} , Ψ_0^O , Ψ_0^Y , denote the harmonic contributions of Ce^{4+} , O^{2-} , Y^{3+} ions to the free energies with the general formula as $\Psi_0 = 3N\theta \left[x + \ln(1 - e^{-2x}) \right]$, and U_0^{Ce} , U_0^O represent the sums of effective pair interaction energies of Ce^{4+} , O^{2-} ions, respectively, in $CeO_{2-x/2}$ system, and U_0^Y represents the sum of effective pair interaction potentials of Y^{3+} ions in $Ce_{1-x}Y_xO_{2-x/2}$ system. It is noted that the presence of oxygen vacancies impacts strongly on the interaction potentials of Ce^{4+} , O^{2-} , Y^{3+} ions. Based on probability theory, the total interaction potentials of Ce^{4+} , O^{2-} and Y^{3+} ions in $CeO_{2-x/2}$ and $Ce_{1-x}Y_xO_{2-x/2}$ systems, respectively, taking into account the role of oxygen vacancies can be determined as

$$U_0^{Ce} = \frac{N_{Ce}}{2} \left(\sum_i b_i^{Ce-Ce} \varphi_{i0}^{*Ce-Ce} + \left(1 - \frac{N_{va}}{2N} \right) \sum_i b_i^{Ce-O} \varphi_{i0}^{*Ce-O} \right), \quad (6)$$

$$U_0^o = \frac{N_o}{2} \left(\sum_i b_i^{o-ce} \phi_{i0}^{*o-ce} + \left(1 - \frac{N_{va}}{2N-1} \right) \sum_i b_i^{o-o} \phi_{i0}^{*o-o} \right), \quad (7)$$

$$U_0^Y = \frac{N_Y}{2} \left(\frac{N_{Ce}}{N-1} \sum_i b_i^{Y-ce} \phi_{i0}^{*Y-Y} + \frac{N_Y-1}{N-1} \sum_i b_i^{Y-Y} \phi_{i0}^{*Y-Y} + \left(1 - \frac{N_{va}}{2N} \right) \sum_i b_i^{Y-o} \phi_{i0}^{*Y-o} \right), \quad (8)$$

with b_i^{X-ce} (or b_i^{X-o} , or b_i^{X-Y}) is the number of the i -th nearest-neighbor sites relative to X ion ($X = Ce^{4+}$, O^{2-} , Y^{3+}) that Ce^{4+} (or O^{2-} , or Y^{3+}) ions can occupy, and ϕ_{i0}^{*X-ce} (or ϕ_{i0}^{*X-o} , or ϕ_{i0}^{*X-Y}) is the interaction potential between the 0-th X ion and a Ce^{4+} (or O^{2-} , or Y^{3+}) ion at the i -th nearest-neighbor sites relative to this X ion, respectively. In $CeO_{2-x/2}$ and $Ce_{1-x}Y_xO_{2-x/2}$ systems with fluorite structure, the interaction potential between the i -th and the j -th ions includes the electrostatic Coulomb potential and Buckingham potential including the short-range interactions

$$\phi_{ij}(r) = \frac{q_i q_j}{r} + A_{ij} \exp\left(-\frac{r}{B_{ij}}\right) - \frac{C_{ij}}{r^6}, \quad (9)$$

where q_i and q_j are the charges of the i -th and the j -th ions, r is the distance between them and the parameters A_{ij} , B_{ij} and c are empirically determined (listed in Table 1).

Table 1. The parameters of the Buckingham potential in $Ce_{1-x}Y_xO_{2-x/2}$ system [11].

Interaction	A_{ij}/eV	$B_{ij}/\text{\AA}$	$C_{ij}/eV (\text{\AA}^6)$
$O^{2-} - O^{2-}$	9547.96	0.2192	32.00
$Ce^{4+} - O^{2-}$	1809.68	0.3547	20.40
$Y^{3+} - O^{2-}$	1766.4	0.3385	19.43

Since pressure P is determined by

$$P = - \left(\frac{\partial \Psi}{\partial V} \right)_T = - \frac{a}{3V} \left(\frac{\partial \Psi}{\partial a} \right)_T, \quad (10)$$

from Eq.(1), it is easy to take out an equation of state of $Ce_{1-x}Y_xO_{2-x/2}$ system at temperature $T = 0K$ and pressure P

$$Pv = -a \left\{ C_{Ce} \left[\frac{1}{6} \frac{\partial u_0^{Ce}}{\partial a} + \frac{\hbar \omega_{Ce}}{4k_{Ce}} \frac{\partial k_{Ce}}{\partial a} \right] + \frac{x}{3} \left[\frac{1}{6} \frac{\partial u_0^Y}{\partial a} + \frac{\hbar \omega_Y}{4k_Y} \frac{\partial k_Y}{\partial a} \right] + C_O \left[\frac{1}{6} \frac{\partial u_0^O}{\partial a} + \frac{\hbar \omega_O}{4k_O} \frac{\partial k_O}{\partial a} \right] - \frac{x}{18} \frac{\partial u_0^{Zr}}{\partial a} \right\}. \quad (11)$$

with v là the atomic volume.

The average nearest-neighbor distance of $\text{Ce}_{1-x}\text{Y}_x\text{O}_{2-x/2}$ system at temperature $T = 0\text{K}$ and pressure P , $r_1(P,0)$ can be derived by numerically solving the equation of state Eq.(11). Then the average nearest-neighbor distance at temperature T and pressure P can be written as

$$r_1(P,T) = r_1(P,0) + C_{\text{Ce}}y_0^{\text{Ce}} + C_{\text{Y}}y_0^{\text{Y}} + C_{\text{O}}y_0^{\text{O}}, \quad (12)$$

with y_0^{Ce} , y_0^{Y} and y_0^{O} are the displacements of Ce^{4+} , Y^{3+} and O^{2-} ions from the equilibrium position in the crystal lattice

$$y_0^{\text{Ce}} \approx \sqrt{\frac{2\gamma_{\text{Ce}}\theta^2}{3k_{\text{Ce}}^3} A_{\text{Ce}}}, \quad y_0^{\text{Y}} \approx \sqrt{\frac{2\gamma_{\text{Y}}\theta^2}{3k_{\text{Y}}^3} A_{\text{Y}}}, \quad (13)$$

$$y_0^{\text{O}} = \sqrt{\frac{2\gamma_{\text{O}}\theta^2}{3K_{\text{O}}^3} A_{\text{O}}} - \frac{\beta_{\text{O}}}{3\gamma_{\text{O}}} + \frac{1}{K_{\text{O}}} \left(1 + \frac{6\gamma_{\text{O}}^2\theta^2}{K_{\text{O}}^4} \right) \left[\frac{2\gamma_{\text{O}}\theta}{3k_{\text{O}}^2} (x \coth x - 1) - \frac{2\beta_{\text{O}}^2}{27\gamma_{\text{O}}k_{\text{O}}} + \frac{1}{3} \right], \quad (14)$$

where parameters A_{Ce} , A_{Y} , A_{O} are determined as Ref.[14]. The lattice constant of $\text{Ce}_{1-x}\text{Y}_x\text{O}_{2-x/2}$ system is then can be defined in relation to the average nearest-neighbor distance as $a(P,T) = 4/\sqrt{3}r_1(P,T)$.

Young's modulus is a mechanical parameter to measure the stiffness of solid materials. In previous study, the Young's modulus E of CeO_2 crystal was given by V.V Hung *et al.* [6]

$$E = \frac{\partial \sigma}{\partial \varepsilon} = \frac{1}{v} \frac{\partial^2 \Psi}{\partial \varepsilon^2}, \quad (15)$$

with ε is the strain, σ denotes the stress.

From Eqs.(1) and (15), it is easy to derive the explicit expression of Young's modulus in the harmonic approximation as

$$E = E_{\text{CeO}_{2-x/2}} + \frac{v}{3v} \left(-\frac{\partial^2 u_0^{\text{Ce}}}{\partial \varepsilon^2} + \frac{\partial^2 \Psi_{\text{Y}}}{\partial \varepsilon^2} \right), \quad (16)$$

where

$$E_{\text{CeO}_{2-x/2}} = \frac{1}{v} \frac{\partial^2 \Psi_{\text{CeO}_{2-x/2}}}{\partial \varepsilon^2}, \quad (17)$$

$$\frac{\partial^2 u_0^{\text{Ce}}}{\partial \varepsilon^2} = 4a_0^2 \frac{\partial^2 u_0^{\text{Ce}}}{\partial a^2} + 2a_0 \frac{\partial u_0^{\text{Ce}}}{\partial a}, \quad (18)$$

$$\frac{\partial^2 \Psi_{\text{Y}}}{\partial \varepsilon^2} = 4a_0 \left\{ \frac{\partial^2 u_0^{\text{Y}}}{\partial a^2} + \frac{3\hbar\omega_{\text{Y}}}{4k_{\text{Y}}} \left[\frac{\partial^2 k_{\text{Y}}}{\partial a^2} - \frac{1}{2k_{\text{Y}}} \left(\frac{\partial k_{\text{Y}}}{\partial a} \right)^2 \right] \right\} + 2a_0 \left\{ \frac{\partial u_0^{\text{Y}}}{\partial a} + \frac{3}{4k_{\text{Y}}} \hbar\omega_{\text{Y}} \coth x_{\text{Y}} \frac{\partial k_{\text{Y}}}{\partial a} \right\}. \quad (19)$$

The isothermal bulk modulus K and shear modulus G can be derived using the following relations

$$K = \frac{E}{3(1-2\nu)}, \quad (20)$$

$$G = \frac{E}{2(1+\nu)}, \quad (21)$$

where ν is Poisson's ratio related to the stability of crystal under shear deformation. In this study, the value of Poisson's ratio is assumed to be 0.33 in accordance with experiment [1].

2.2. Results and discussion

The lattice constant of YDC crystal at the different dopant concentrations is presented in Fig. 1. One can see that the lattice constant decreases with the increasing dopant concentration. This dependence arises mainly from the creation of the oxygen vacancies that leads to a lattice contraction. Using empirical equations, N. Kim *et al.* [7] showed a linear relationship between the lattice constant and the dopant concentration in fluorite-structure oxide solid solutions. Fig.1 shows that SMM results at the room temperature are in good agreement with the results obtained from other theories [2, 27] and experiments [7, 27].

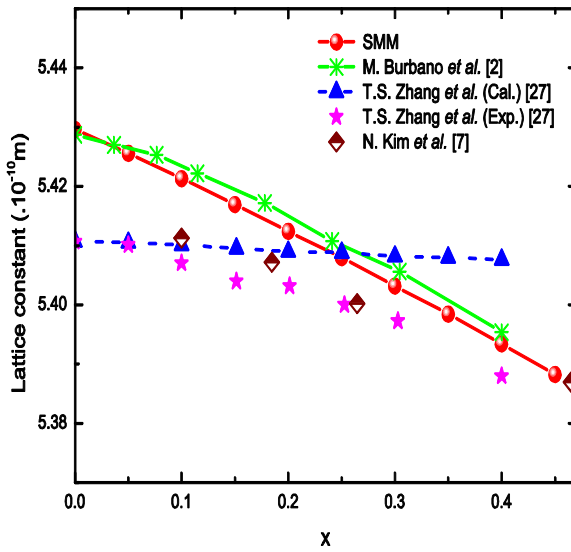


Figure 1. The dopant concentration dependence of lattice constant at $T = 300\text{K}$. The other theoretical [2, 27] and experimental [7, 27] results are presented for comparison.

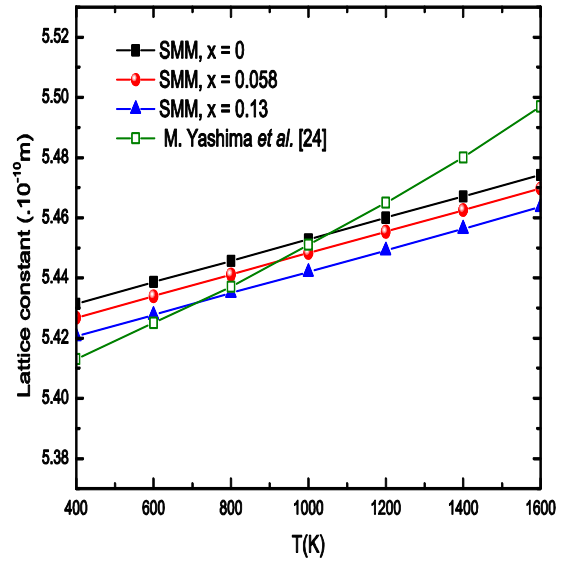


Figure 2. The temperature dependence of lattice constant at various dopant concentrations, $x = 0$, $x = 0.06$, $x = 0.13$. The experimental results [24] are presented for comparison.

In Fig. 2, we compare the lattice constant at pressure $P = 0$ using the SMM with the experimental results (in the case of pure CeO_2) [24] for temperature range $T = 400\text{K} - 1600\text{K}$. The calculated lattice constants by the present theory are slightly larger than the experimental values for temperature range $T = 400\text{K} - 800\text{K}$, and slightly smaller than the experimental values for temperature range $T = 800\text{K} - 1600\text{K}$, but overall features are in good agreement.

with the experimental results [24]. The predicted zero-pressure lattice constant $a(0,400\text{K}) = 5.4314 \text{ \AA}$ agrees within 0.4% with the corresponding experimental value 5.413 \AA .

In Fig. 3, we compare the SMM results of lattice constant at the room temperature and various pressures with the experimental results (in the case $x = 0$). Fig. 3 also shows the experimental lattice constants of pure CeO_2 [5, 22] as functions of the pressure. The pressure dependence of the lattice constant at the different dopant concentrations is similar for a wide pressure range. Our SMM theory predicts that the lattice constant of YDC crystal decreases rapidly with the pressure. The obtained results are in agreement with those measured by experiments for pure CeO_2 [5, 22]. The predicted zero-pressure lattice constant $a(0,300\text{K}) = 5.4291 \text{ \AA}$ agrees within 0.3 % with the corresponding experimental value 5.411 \AA .

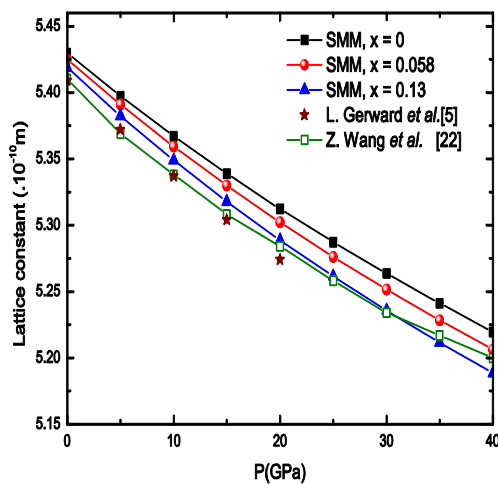


Figure 3. The pressure dependence of lattice constant at various dopant concentrations, $x = 0, x = 0.06, x = 0.13$. The experimental results [5, 22] are presented for comparison.

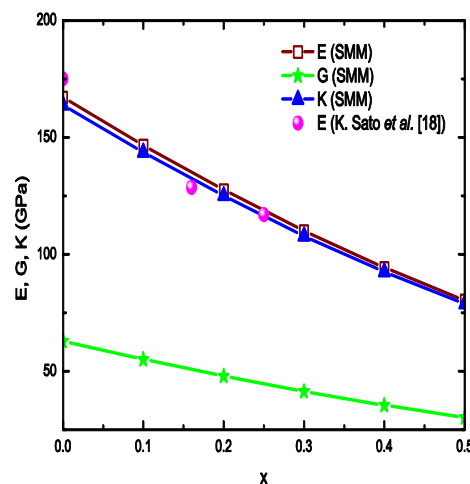


Figure 4. The dopant concentration dependence of Young's, bulk, shear moduli at the room temperature. The experimental results [18] are presented for comparison.

Fig. 4 shows how the dopant concentration dependence of the Young's E , bulk K , and shear moduli G . One can see that all YDC with different dopant concentrations has lower Young's E , bulk K , and shear moduli values than those of pure ceria ($x = 0$). The presence of oxygen vacancies related to the replacement of Ce^{4+} by Y^{3+} ions decreases the binding energy between cations and anions near the oxygen vacancies. Consequently, the elastic moduli decrease as the dopant concentration increases. The SMM results of bulk modulus K are in good agreement with the experimental results using scanning electron microscopy and small specimen technique [18]. The temperature dependence of Young's, bulk, shear moduli is given in Fig. 5. The SMM results of the Young's, bulk and shear moduli with $x = 0.2$ decrease gradually with the increasing temperature. Accordingly, YDC crystal becomes easier to elongate at high temperatures. The rapid reduction in the elastic moduli indicates the stronger anharmonicity contributions of the thermal lattice vibrations at high temperatures.

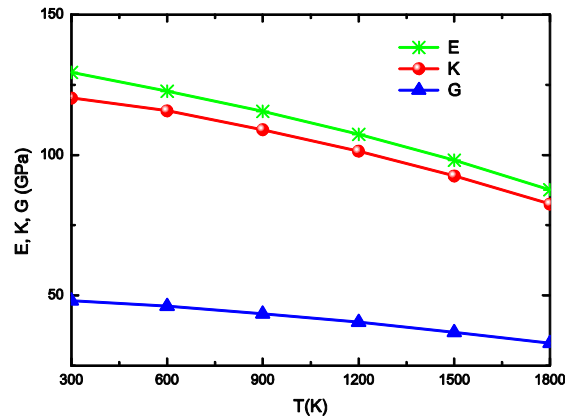


Figure 5. The temperature dependence of Young's, bulk, shear moduli of YDC crystal.

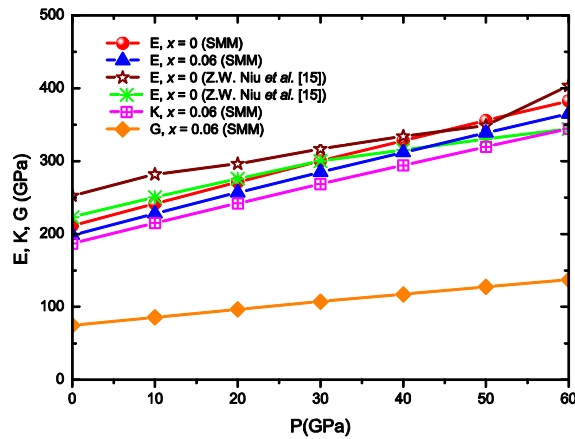


Figure 6. The pressure dependence of Young's, bulk, shear moduli at various dopant concentrations, $x = 0$, $x = 0.06$. The results using LDA and LDA+U methods [15] are presented for comparison.

In Fig. 6, the calculated Young's, bulk and shear moduli with $x = 0.06$ are plotted as functions of pressure P . It is clearly seen that the Young's, bulk and shear moduli depend sensitively on the pressure. The lattice constant decreases due to an increase of pressure, therefore the elastic moduli become larger. The obtained results of Young's modulus using the local-density approximation (LDA) and LDA+U methods [15] are also shown for comparison with the SMM result for CeO_2 crystal. N. Wei *et al.* [23] explained that the material with larger Young's modulus responds to the more covalent feature of the material. The Young's modulus increases linearly with the increase of the pressure, which means that CeO_2 and YDC crystals become more stiff under the pressure.

3. CONCLUSION

The lattice constant and elastic moduli of YDC crystal are investigated using the SMM including the anharmonicity effects of thermal lattice vibrations. The SMM calculations are also performed using the Buckingham potential for YDC crystal with fluorite structure. The lattice constant and elastic moduli are calculated as functions of the dopant concentration,

temperature, and pressure. The influences of dopant concentration, temperature, and pressure on the lattice constant and elastic moduli have been studied in detail. Our results are in good agreement with previous experiments and several theoretical calculations.

REFERENCES

1. A. Atkinson and A. Selcuk (2000), "Mechanical behaviour of ceramic oxygen ion-conducting membranes", *Solid State Ionic*. **134**, pp.59.
2. A. Tschope, W. Liu, M. Flytzanistephanopoulos, and J. Y. Ying (1995), "Redox activity of nonstoichiometric cerium oxide based nanocrystalline catalysts", *Journal of Catalysis*. **157**, pp.42.
3. D. Marrocchelli, S.R. Bishop, H.L. Tuller and B. Yildiz (2012), "Understanding Chemical Expansion in Non-Stoichiometric Oxides: Ceria and Zirconia Case Studies", *Adv. Funct. Mater.* **22**, pp.1958-1965.
4. E. Wachtel and I. Lubomirsky (2011), "The elastic modulus of pure and doped ceria", *Scripta Materialia*. **65**, pp.112.
5. F. Zhang, S.-W. Chan, J.E. Spanier, E. Apak, Q. Jin, R.D. Robinson and I.R. Herman (2002), "Cerium oxide nanoparticles: Size-selective formation and structure analysis", *Appl. Phys. Lett.* **80**, pp.127.
6. J.L.M. Rupp, C. Solenthaler, P. Gasser, U.P. Muecke and L.J. Gauckler (2007), "Crystallization of amorphous ceria solid solutions", *Acta Mater.* **55**, pp.3505.
7. J.R. McBride, K.C. Hass, B.D. Poindexter and W.H. Weber (1994), "Raman and x-ray studies of $Ce_{1-x}RE_xO_{2-y}$, where RE = La, Pr, Nd, Eu, Gd, and Tb", *J. Appl. Phys.* **76**, pp.2435.
8. K. Muthukumar, R. Bokalawela, T. Mathews and S. Selladurai (2007), "Determination of dopant of ceria system by density functional theory", *J. Mater. Sci.* **42**, pp.7461.
9. K. Sato, H. Yugami and T. Hashida (2004), "Effect of rare-earth oxides on fracture properties of ceria ceramics", *Journal of Materials Sciences*. **39**, pp.5765.
10. L. Gerward, J. Staun Olsen, L. Petit, G. Vaitheeswaran, V. Kanchana and A. Svane (2005), "Bulk modulus of CeO_2 and PrO_2 - An experimental and theoretical study", *Journal of Alloys and Compounds*. **400**, pp.56.
11. L.T. Lam, V.V. Hung, B.D. Tinh (2019), "Investigation of electrical properties of Ytria-doped Ceria and Ytria-Stabilized Zirconia by statistical moment method", *Journal of the Korean Physical Society*. **75** (4), pp.293.
12. L.T. Lam, V.V. Hung, N.T. Hai (2019), "Effect of temperature on electrical properties of Ytria-doped Ceria and Ytria-stabilized Zirconia", *HNUE Journal of Science*. **64** (6), pp.68.
13. M. Burbano, S.T. Norberg, S. Hull, S.G. Eriksson, D. Marrocchelli, P.A. Madden and G.W. Watson (2012), "Oxygen Vacancy Ordering and the Conductivity Maximum in Y_2O_3 -Doped CeO_2 ", *Chem. Mater.* **24**, pp.222.
14. M. Yashima, D. Ishimura, Y. Yamaguchi, K. Ohoyama and K. Kawachi (2003), "High-temperature neutron powder diffraction study of cerium dioxide CeO_2 up to 1770K", *Chemical Physics Letters*. **372**, pp.784.
15. M.-Y. Cheng, D.-H. Hwang, H.-S. Sheu and B.-J. Hwang (2008), "Formation of $Ce_{0.8}Sm_{0.2}O_{1.9}$ nanoparticles by urea-based low-temperature hydrothermal process", *Journal of Power Sources*. **175**, pp.137.
16. N. Kim and J.F. Stebbins (2007), "Vacancy and Cation Distribution in Ytria-Doped Ceria: An

- ⁸⁹Y and ¹⁷O MASNMR Study”, *Chem. Mater.* 19, pp.5742.
17. N. Wei, X. Zhang, C. Zhang, S. Hou and Z. Zeng (2015), “First-principles investigations on the elastic and thermodynamic properties of cubic ZrO₂ under high pressure”, *International Journal of Modern Physics*. C26, pp.1550056.
 18. P. Li, I-W. Chen, J.E. Penner-Hahn and T.-Y. Tien (1991), “X-ray Absorption Studies of Ceria with Trivalent Dopants”, *J. Am. Ceram. Soc.* 74, pp.958
 19. P.-L. Chen and I.W. Chen (1994), “Role of Defect Interaction in Boundary Mobility and Cation Diffusivity of CeO₂”, *J. Am. Ceram. Soc.* 77, pp.2289.
 20. R. Pornprasertsuk, P. Ramanarayanan, C. B. Musgrave, and F. B. Prinz (2005), “Predicting ionic conductivity of solid oxide fuel cell electrolyte from first principles”, *Journal of Applied Physics*. 98, pp.103513.
 21. S. Vyas, R.W. Grimes, D.H. Gay and A.L. Rohl, *J. Chem. Soc.* (1998), “Structure, Stability and Morphology of Stoichiometric Ceria Crystallites”, *Faraday Trans.* 94 (3), pp.427.
 22. T.S. Zhang, J. Ma, H.T. Huang, P. Hing, Z.T. Xia, S.H. Chan and J.A. Kilner (2003), “Effects of dopant concentration and aging on the electrical properties of Y-doped ceria electrolytes”, *Solid State Sciences*. 5, pp.1505.
 23. V.G. Zavodinsky (2004), “The mechanism of ionic conductivity in stabilized cubic zirconia”, *Physics of the Solid State*. 46, pp.453.
 24. V.V. Hung, L.T.M. Thanh, “Study of elastic properties of CeO₂ by statistical moment method”, *Physica B*. 406 (2011), pp.4014.
 25. Z. Wang, Y. Zhao, D. Schiferl, C.S. Zha and R.T. Downs (2004), “Pressure induced increase of particle size and resulting weakening of elastic stiffness of nanocrystals”, *J. Appl. Phys.* 85, pp.124.
 26. Z.-P. Li, T. Mori, F. Ye, D. Ou, G. J. Auchterlonie, J. Zou, and J. Drennan (2012), “Cerium-Reduction-Induced Defects Clustering, Ordering, and Associated Microstructure Evolution in Yttrium-Doped Ceria”, *J. Phys. Chem. C*. 116, pp.5435.
 27. Z.W. Niu, B. Zhu, Y. Cheng, R.N. Song and G.F. Ji (2014), “Elastic and electronic properties of cubic cerium oxide under pressure via first principles”, *International Journal of Modern Physics*. B28, pp.1450070.

NGHIÊN CỨU HẰNG SỐ MẠNG VÀ MÔ ĐUN ĐÀN HỒI CỦA TINH THỂ CERIA PHA TẠP YTTRIA BẰNG PHƯƠNG PHÁP THỐNG KÊ MÔMEN

Tóm tắt: Trong nghiên cứu này, chúng tôi đã phát triển hình thức luận dựa vào phương pháp thống kê momen để nghiên cứu hằng số mạng và môđun đàn hồi của tinh thể Ceria pha tạp Yttria có tính đến các ảnh hưởng phi điều hoà của các dao động mạng tinh thể. Hằng số mạng, môđun đàn hồi được tính toán là các hàm của nồng độ tạp chất, nhiệt độ và áp suất. Sử dụng thể Buckingham, chúng tôi tính toán môđun đàn hồi với nhiệt độ lên tới 1800K và áp suất lên tới 60 GPa. Các tính toán của chúng tôi được so sánh với các kết quả lý thuyết và thực nghiệm.

Từ khóa: Hằng số mạng, môđun đàn hồi, tinh thể ceria pha tạp yttria.